ChemComm

Chemical Communications

www.rsc.org/chemcomm

Volume 49 | Number 9 | 30 January 2013 | Pages 833–932

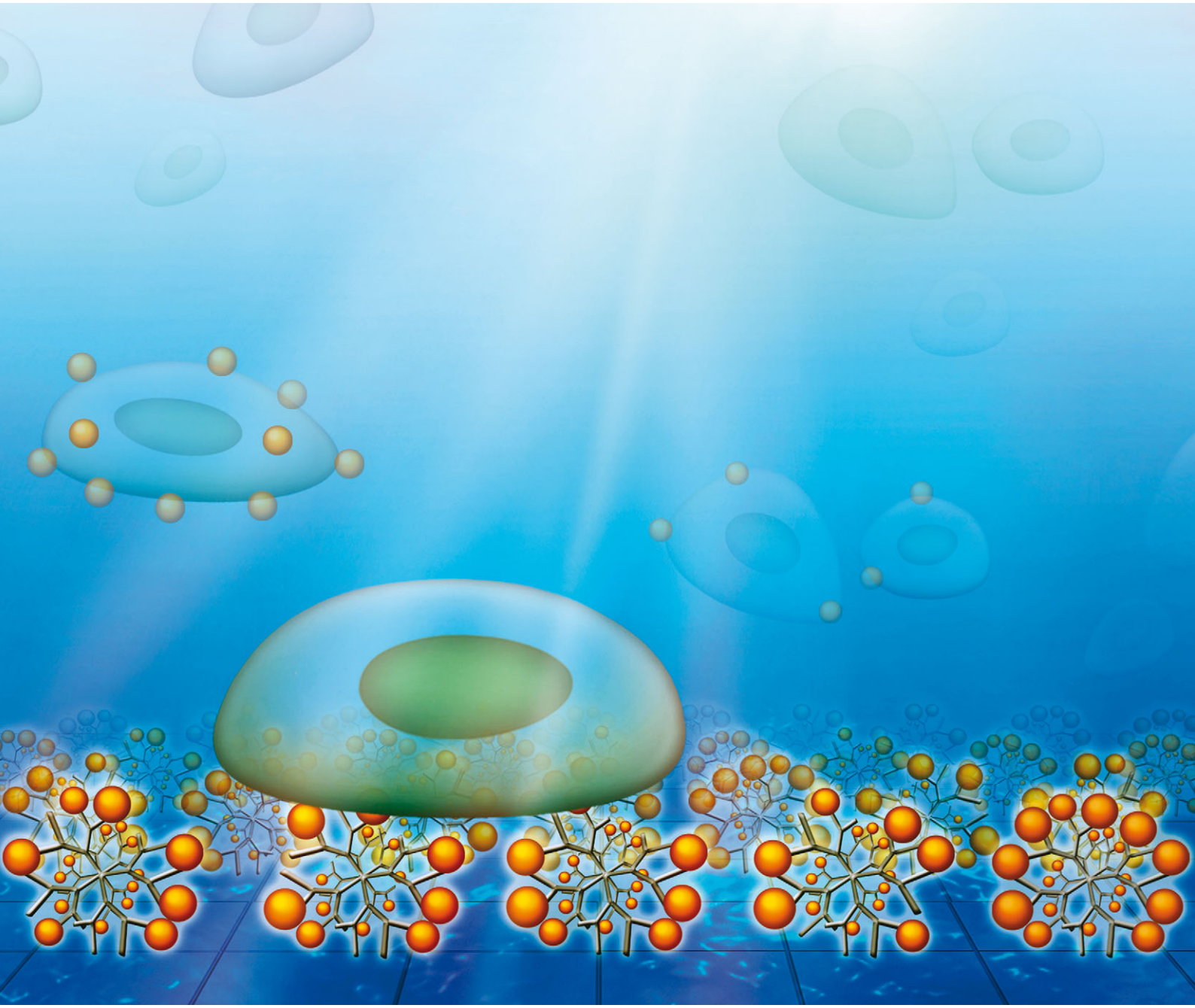

ISSN 1359-7345

RSC Publishing

COMMUNICATION

Lin Ding, Huangxian Ju *et al*.

In situ tracing of cell surface sialic acid by chemoselective recognition to unload gold nanocluster probe from density tunable dendrimeric array

ChemComm

RSC Publishing

COMMUNICATION

In situ tracing of cell surface sialic acid by chemoselective recognition to unload gold nanocluster probe from density tunable dendrimeric array†

Cite this: *Chem. Commun.*, 2013, **49**, 862

Received 25th October 2012,
Accepted 30th November 2012

DOI: 10.1039/c2cc37761f

www.rsc.org/chemcomm

Yunlong Chen,[a] Lin Ding*[ab] and Huangxian Ju*[a]

A density tunable dendrimeric array was designed for assembly of a gold nanocluster probe, which was unloaded by its chemoselective recognition to cell surface sialic acid for *in situ* tracing of sialic acid density.

Glycan-involved recognition mediates a variety of important biological processes.[1] The recognition events in nature often occur through multivalent formatting.[2] To match the binding sites of the receptor, proper spatial presentation of glycans on the cell surface, in the aspects of density, spacing, orientation, flexibility and overall architecture, is critical for efficient recognition.[3] Among these factors, density has been considered to have a major impact.[4] Changes in glycan density may lead to switching in binding avidity and selectivity.[5,6] Thus, exploration of strategies for monitoring glycan density to provide information of cell surface interaction is one of the current challenges to functional glycomics investigation.

Many methods based on mass spectrometry and chromatography *etc*. have been developed for glycomic detection.[7] Some microscopic and electrochemical approaches based on biological or chemoselective recognition have also shown great promise for *in situ* analysis of glycans on living cells.[8] However, these techniques are unable to provide direct information of the spatial organization feature of cell surface glycans. Although glycan array-based techniques can be used to evaluate glycan density-dependent binding properties,[9] they fail to correlate these binding process directly with cell surface glycan density.

Herein, a density tunable dendrimeric array was designed for *in situ* tracing of cell surface glycan density, using terminally-expressed sialic acids (SAs) as the target, which play crucial roles in a wide variety of physiological and pathological processes.[10] The assay system consisted of a slide modified with poly(amidoamine) (PAMAM) dendrimer at a series of tunable densities to electrostatically assemble 3-aminophenylboronic acid (APBA) functionalized gold nanoclusters (AuNCs) as luminescent probes. The probe could bind SA groups on the cell surface by a chemoselective covalent linkage between APBA and SAs at pH 7.4 (Scheme 1).[11] Using BGC-823 cells as the model, through covalently binding to the cells, the electrostatically adsorbed APBA-AuNC probe could be unloaded from the dendrimer-modified slide, leading to a decrease of fluorescence intensity (FI) of the probe on the slide. The amount of unloaded probe from the slide depended on the dendrimer density, cell number and the expression extent of SAs on

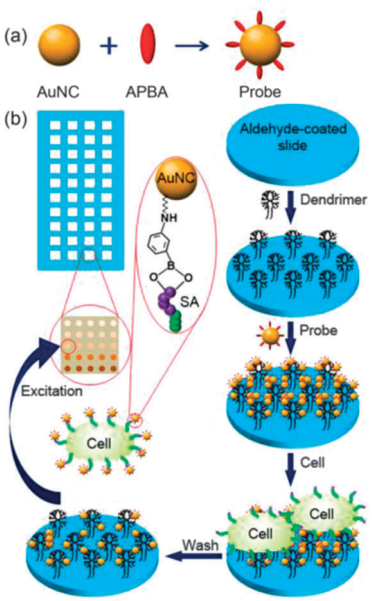

Scheme 1 Schematic illustration of (a) probe fabrication and (b) assay process.

[a] *State Key Laboratory of Analytical Chemistry for Life Science, Department of Chemistry, Nanjing University, Nanjing 210093, P.R. China. E-mail: hxju@nju.edu.cn, dinglin@nju.edu.cn; Fax: +86 25 83593593; Tel: +86 25 83593593*

[b] *High-Tech Research Institute of Nanjing University, Changzhou 213164, P.R. China*

† Electronic supplementary information (ESI) available: Additional experimental details, characterization of probe and dendrimeric array, demonstration of recognition specificity and cell viability, and optimization of detection conditions. See DOI: 10.1039/c2cc37761f

the cell surface. The dendrimer density determined the spatial matching extent between SA epitopes and the probe-adsorbed dendrimer, which could be reflected by the unloading efficiency, that is the FI change rate of probe remaining on the dendrimer-modified slide with increasing cell concentration (Scheme S1, ESI†). At different dendrimer densities, the FI change rate was different, which produced an inflection point on the plot of change rate *vs.* dendrimer density. The inflection point could be considered as the critical point of spatial matching extent to estimate the SA density on the cell surface.

AuNCs possess several advantages for bioanalysis, such as bright emission, excellent photostability and good biocompatibility with low steric hindrance and fast kinetics.[12] Here glutathione (GSH) coated AuNCs were prepared using reduced GSH as reducing and stabilizing agent.[13] The AuNCs were then functionalized with APBA by a carbodiimide chemistry. The obtained APBA-AuNCs as signal reporter probes combined the SA chemoselective recognition capability of APBA and minimizing nonspecific protein/cell adsorption of GSH.[14] The UV-vis spectra of both AuNCs and APBA-AuNCs did not exhibit obvious surface plasmon absorption, while their fluorescence spectra exhibited a maximum emission at 574 nm (Fig. S1a and b, ESI†). The stronger emission of APBA-AuNCs could be attributed to the better dispersion and increased homogeneity after APBA conjugation, as verified by TEM images (Fig. S1d and e, ESI†). The conjugation also led to a change of zeta potentials from −1.16 to −20.7 mV (Fig. S1c, ESI†), indicating more negative charged groups. The appearance of a B 1s peak in the XPS spectrum further verified the successful conjugation process (Fig. S1f, ESI†).

Nanoscale PAMAM dendrimer possesses a defined cluster configuration with small size and compact spherical geometry.[15] This work used a density tunable PAMAM (G5) dendrimer array to control the absorption of APBA-AuNC probe and the ability of cells to unload the probe from dendrimer modified microspots. The dendrimeric monolayers were prepared by printing different concentrations of amino terminated-PAMAM dendrimer on an aldehyde-coated glass slide with five replicate spots in a panel. The diameter of each spot was 200 μm. After the dendrimeric array was subjected to incubation with BSA to block unreacted aldehyde group, the negatively charged APBA-AuNC was adsorbed on the positively charged dendrimer surface.[16] The step-by-step construction was verified by atomic force microscopic characterization (Fig. S2, ESI†). The probe-assembled array were then incubated with different concentrations of cell suspensions. After a wash step, the fluorescent images of remaining probe on dendrimer spots were recorded under fixed scanning conditions. For maximum reflection of the signal change, the red channel intensity (I) of given spots was read using Photoshop software to represent the FI.

The specific recognition of the APBA on the probe to cell surface SAs was verified by the strong fluorescence from the cells that were incubated with APBA-AuNC adsorbed dendrimer solution (Fig. S3, ESI†). In the absence of APBA, fluorescence emission was not observed, indicating very little non-specific adsorption of AuNCs toward cells. To verify the participation of SAs in the specific recognition, sialidase was used to cleave the SA groups from the cell surface. Compared with untreated cells, the treated cells only showed very small change of I upon the unloading process (Fig. S4, ESI†). This also implied that the decrease of I was attributed to the unloading of the probe from dendrimer array by the specific binding between SAs and APBA.

To choose a suitable dendrimer concentration for array preparation, a series of dendrimer spots with varying PAMAM concentration were subjected to saturated adsorption of APBA-AuNCs. The I value increased with increasing dendrimer concentration and reached a steady value at 1.75 mg mL^{-1} (Fig. S5a, ESI†). Thus the optimal concentration range of PAMAM was 0.5–1.75 mg mL^{-1}. The maximum density achievable corresponded to the maximum capacity of the surface, at which the dendrimer was most close-packed. From the 5.4 nm diameter of dendrimer, the maximum dendrimer density was estimated to be 3.96×10^4 μm^{-2}. Considering that the I value was proportional to the dendrimer density, other dendrimer densities were obtained from the I values to be 3.69×10^4, 3.19×10^4, 2.47×10^4 and 1.73×10^4 μm^{-2}. The probe concentration, adsorption time of probe and unloading time of cells were optimized by examining their effects on I value. The optimal values were 0.1 mmol, 10 min and 1 h, respectively (Fig. S5b–d, ESI†). Furthermore, MTT assay verified that the assay process did not affect the viability of cells (Fig. S6, ESI†).

Under the optimal conditions, a series of APBA-AuNC adsorbed panels at five dendrimer densities were incubated with cells of different concentration to unload the probe from the spots. After the washing step, no cells were adsorbed on the dendrimer, which was observed under microscopy. The fluorescence images showed obvious decrease of fluorescent signal at dendrimer spots. The completely black background indicated that no probe was adsorbed on dendrimer-absent areas (Fig. 1a).

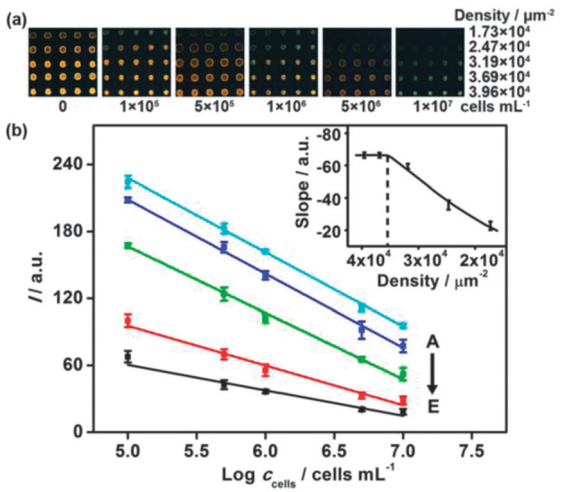

Fig. 1 (a) Fluorescent images of APBA-AuNC adsorbed dendrimeric array with different dendrimer densities after unloading by cells at different concentrations. (b) Plots of I *vs.* logarithm of cell concentration at dendrimer densities of 3.96×10^4, 3.69×10^4, 3.19×10^4, 2.47×10^4 and 1.73×10^4 μm^{-2} (from A–E). Inset: plot of slope *vs.* dendrimer density.

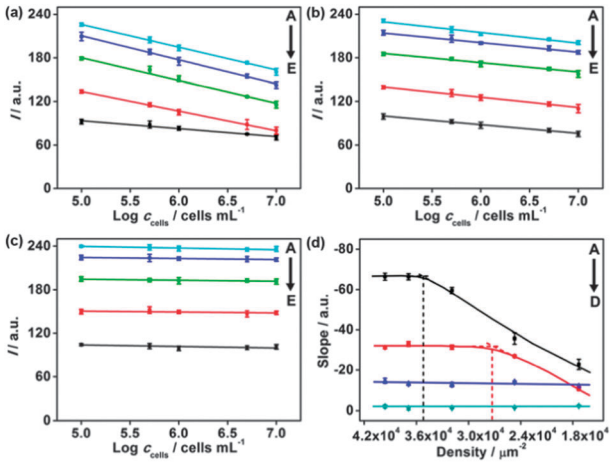

Fig. 2 Plots of *I vs.* logarithm of cell concentration at dendrimer densities of 3.96×10^4, 3.69×10^4, 3.19×10^4, 2.47×10^4 and 1.73×10^4 μm^{-2}, respectively (from A–E) using cells treated with sialidase for (a) 10 min, (b) 20 min and (c) 4 h. (d) Plots of slope *vs.* dendrimer density using untreated cells (A) and cells treated with sialidase for 10 min (B), 20 min (C) and 4 h (D) in the assay process.

Along with increasing dendrimer density or decreasing cell concentration, greater fluorescent signal could be observed. The *I* value was found to be proportional to the logarithmic value of BGC cell concentration in the detection range at each dendrimer density (Fig. 1b). The different slopes indicated the change rate of *I* with increasing cell concentration depended on dendrimer density. The plot of slope *vs.* dendrimer density showed the dependence (inset in Fig. 1b). At the densities less than 3.53×10^4 μm^{-2}, the slope decreased.

The decrease of fluorescent signal resulted from the unloading of APBA-AuNC probe adsorbed on dendrimer. It could be reasonably speculated that when the dendrimer density was greater than the cell surface SA density, SAs on the cell surface could efficiently unload the probe, so the change rate of *I* could remain a constant value until the density reached the critical value that was equivalent to the SA density on the cell surface. Then the dendrimer density of 3.53×10^4 μm^{-2} occuring the inflection point for slope change could approximately correspond to the SA density on the cell surface. Assuming the average diameter of BGC-823 cell as 20 μm, this amount of SA on a single cell was consistent with that reported previously.[8c] Different from existing methods for measuring the density of cell surface receptors, which relied on two different recognition pairs,[17] this method required only one kind of recognition pair.

The proposed method enabled to monitor subtle changes of glycan density in response to drugs. Sialidase was selected as the model drug for cleaving SAs. After sialidase treatment, the change of *I* with increasing cell concentration was reduced (Fig. 2a–c). Along with longer treatment time, the plot gradually tended to a flat line. This result demonstrated the decrease of SA expression by sialidase cleaving, and was in agreement with a previous report.[8d] At relatively short treatment time, the plot slope of *I vs.* logarithm of cell concentration showed a correlation to dendrimer density, while this correlation disappeared at longer treatment time due to the low SA density on cell surface, which exceeded the given dendrimer density range (Fig. 2d). When the cells were treated for 10 min, the SA density on the cell surface was measured to be 2.73×10^4 μm^{-2} from the inflection point for the slope change (curve B in Fig. 2d).

In conclusion, a density tunable dendrimeric array-based assay has been developed for *in situ* tracing of cell surface SA density. The detection process uses functionalized gold nanoclusters as probes that show bright luminescence, high glycan selectivity and low non-specific adsorption. This method possesses high throughput, acceptable reproducibility and low cost. This strategy can be further applied for tracking subtle changes of SA density on the cell surface in response to drug treatment. By controlling the density range of dendrimer on the array, broader density range of cell surface SA can be traced. It can be anticipated that this method for cell surface glycan tracing would contribute to progress toward a fundamental understanding of glycan-related biological processes.

We gratefully acknowledge the National Basic Research Program of China (2010CB732400), National Natural Science Foundation of China (21005037, 21135002, 21121091), PhD Fund for Young Teachers (20100091120034), and Natural Science Foundation of Jiangsu (BK2010193).

Notes and references

1 P. H. Seeberger and D. B. Werz, *Nature*, 2007, **446**, 1046–1051.
2 (*a*) J. J. Lundquist and E. J. Toone, *Chem. Rev.*, 2002, **102**, 555–578; (*b*) P. I. Kitov and D. R. Bundle, *J. Am. Chem. Soc.*, 2003, **125**, 16271–16284.
3 Y. L. Zhang, Q. Li, L. G. Rodrigue and J. C. Gildersleeve, *J. Am. Chem. Soc.*, 2010, **132**, 9653–9662.
4 C. F. Brewer, M. C. Miceli and L. G. Baum, *Curr. Opin. Struct. Biol.*, 2002, **12**, 616–623.
5 T. K. Dam and C. F. Brewer, *Glycobiology*, 2009, **20**, 270–279.
6 N. Horan, L. Yan, H. Isobe, G. M. Whitesides and D. Kahne, *Proc. Natl. Acad. Sci. U. S. A.*, 1999, **96**, 11782–11786.
7 K. T. Pilobello and L. K. Mahal, *Curr. Opin. Chem. Biol.*, 2007, **11**, 300–305.
8 (*a*) K. L. Hsu, K. T. Pilobello and L. K. Mahal, *Nat. Chem. Biol.*, 2006, **2**, 153–157; (*b*) W. Cheng, L. Ding, S. J. Ding, Y. B. Yin and H. X. Ju, *Angew. Chem., Int. Ed.*, 2009, **48**, 6465–6468; (*c*) R. C. Qian, L. Ding, L. Bao, S. J. He and H. X. Ju, *Chem. Commun.*, 2012, **48**, 3848–3850; (*d*) E. Han, L. Ding and H. X. Ju, *Anal. Chem.*, 2011, **83**, 7006–7012.
9 O. Oyelaran and J. C. Gildersleeve, *Curr. Opin. Chem. Biol.*, 2009, **13**, 406–413.
10 W. R. Alley Jr. and M. V. Novotny, *J. Proteome Res.*, 2010, **9**, 3062–3072.
11 A. Matsumoto, H. Cabral, N. Sato, K. Kataoka and Y. Miyahara, *Angew. Chem., Int. Ed.*, 2010, **49**, 5494–5497.
12 L. Shang, S. J. Dong and G. U. Nienhausa, *Nano Today*, 2011, **6**, 401–418.
13 C. Zhou, C. Sun, M. X. Yu, Y. P. Qin, J. G. Wang, M. Kim and J. Zheng, *J. Phys. Chem. C*, 2010, **114**, 7727–7732.
14 M. X. Yu, C. Zhou, J. B. Liu, J. D. Hankins and J. Zheng, *J. Am. Chem. Soc.*, 2011, **133**, 11014–11017.
15 (*a*) S. H. Medina and M. E. H. El-Sayed, *Chem. Rev.*, 2009, **109**, 3141–3157; (*b*) H. M. Ja, A. G. Khyati, S. Jelena, T. E. David and H. Seungpyo, *Angew. Chem., Int. Ed.*, 2011, **50**, 11769–11772.
16 M. El-Sayed, M. F. Kiani, M. D. Naimark, A. H. Hikal and H. Ghandehari, *Pharm. Res.*, 2001, **18**, 23–28.
17 (*a*) J. Matko and M. Edidin, *Methods Enzymol.*, 1997, **278**, 444–462; (*b*) Y. Chen, M. B. O'Donoghue, Y. F. Huang, H. Z. Kang, J. A. Phillips, X. L. Chen, M. C. Estevez, C. Y. J. Yang and W. H. Tan, *J. Am. Chem. Soc.*, 2010, **132**, 16559–16570.

